

STABILITY OF INTERFACIAL WAVES IN ALUMINIUM REDUCTION CELLS

P. A. Davidson and R. I. Lindsay

Department of Engineering, University of Cambridge,
Trumpington Street, Cambridge CB2 1PZ, England

Abstract

We have developed a simple model of reduction cell instabilities which highlights the critical role played by the single grouping $J_o B_z / hH$, where J_o is the current density in the cell, B_z is the vertical component of the background magnetic field and h and H are the depths of electrolyte and aluminium. We discuss the implications of this model for the stability of real cells and suggest means of increasing the stability threshold of cells without reducing their performance.

Introduction

Aluminium is produced by the electrolysis of aluminium oxide in reduction cells. These consist of large carbon blocks (electrodes), between which lie a shallow layer

of liquid aluminium together with a second (lighter) layer of electrolyte. Disturbances are readily triggered at the electrolyte-aluminium interface. These are long wavelength, interfacial gravity waves, modified by the intense magnetic and electric fields which pervade the cell. Under certain conditions these disturbances are observed to grow, disrupting the operation of the cell. (See Figure 1). To some extent the mechanism of this instability is clear. A displacement of the interface inevitably leads to a redistribution of current, \mathbf{J} , within the cell. This is illustrated in Figure 2 where the perturbation in current, \mathbf{j} , is shown.

Excess current is drawn from the anode into the electrolyte at those points where the thickness of the highly resistive electrolyte (cryolite) is reduced, and less current is drawn at points where the cryolite depth is increased. The resulting perturbation in cryolite current is vertical, as

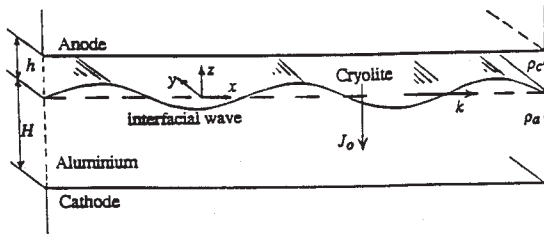


Figure 1: The cell geometry.

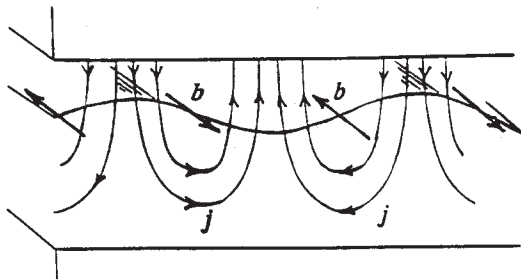


Figure 2: The perturbation in current and magnetic field due to the passage of an interfacial wave.

shown. Since the carbon cathode is much more resistive than the aluminium, these perturbations in vertical current feed into the aluminium but do not penetrate the cathode. Associated with \mathbf{j} there is a perturbation in the magnetic field, \mathbf{b} , which is directed parallel to the wave crests. If \mathbf{J}_0 and \mathbf{B}_0 are the unperturbed current density and magnetic fields, then movement of the interface produces a perturbation in the Lorentz force given by

$$\delta\mathbf{F} = \mathbf{J}_0 \times \mathbf{b} + \mathbf{j} \times \mathbf{B}_0 \quad (1)$$

The question is now whether or not this perturbation in force acts to reinforce the initial disturbance. This question was clarified, for cases where the lateral boundaries of the cell are ignored, by Sneyd[9], Moreau and Ziegler[5], and Davidson[2]. These authors considered the (infinite) interface to be perturbed by *travelling waves*. But these travelling-wave models leave open the question of the influence of the lateral boundaries of the cell. This is particularly important as the waves observed in practice have wavelengths comparable with the lateral dimensions of the cell. It seems probable, therefore, that the observed motions consist of *standing waves*, modified in some way by the electromagnetic forces.

This rather different problem has been tackled by Sele[7], Urata[11], Sneyd and Wang[10], Bojarevics and Romerio[1], and Segatz and Droste[6]. They conclude that the stability characteristics of standing waves are very different to those of the travelling waves investigated earlier. Specifically, the criteria for instability are different in the two cases.

In this paper, we further develop the work of Davidson and Lindsay[3, 4] who derived a new model of the interfacial instability. This not only encompasses the predictions of Sneyd and Wang[10] and Bojarevics and Romerio[1] but also pre-

dicts unstable travelling waves. We also discuss the implications of the model for real cells.

A Simplified Model of a Cell

Our simplified model is shown in Figure 1. The undisturbed depths of cryolite and aluminium are h and H , and the unperturbed current flow is purely vertical and has magnitude J_0 . We use a Cartesian coordinate system, (x, y, z) , where z is vertical and directed upward. The origin for z lies at the undisturbed interface.

The magnetic Reynolds number is small in reduction cells and so Ohm's law simplifies to

$$\begin{aligned} \mathbf{J} &= \sigma \mathbf{E} = -\sigma \nabla \Phi, \\ \nabla^2 \Phi &= 0. \end{aligned} \tag{2}$$

We are concerned only with linear stability, so we consider infinitesimal perturbations of the interface of the form $z_s = \eta(x, y, t)$. The corresponding distributions of \mathbf{J} and \mathbf{B} are

$$\begin{aligned} \mathbf{J} &= \mathbf{J}_0 + \mathbf{j} = -J_0 \hat{\mathbf{e}}_z - \sigma \nabla \phi, \\ \mathbf{B} &= \mathbf{B}_0 + \mathbf{b}. \end{aligned} \tag{3}$$

The boundary conditions on \mathbf{J} arise from the ranking of the electrical conductivities:

$$\sigma_a \gg \sigma_{\text{carbon}} \gg \sigma_c. \tag{4}$$

Here the subscripts 'a' and 'c' refer to the aluminium and cryolite. It is not difficult to show that (4) requires $\phi_c = 0$ on $z = h$ and $\partial \phi_a / \partial z = 0$ on $z = -H$. Here ϕ is the perturbation in the electrostatic potential. The first of the boundary conditions states that the anode potential is fixed, while the second ensures that \mathbf{j} does not penetrate into the cathode blocks.

We shall also assume that the fluid is inviscid, that surface tension can be ignored, and that there is no background motion in the unperturbed state. The last of the three assumptions above is not particularly realistic, but is essential to the stability analysis. That is, it is by no means clear how the analysis could be generalised to include background motion and no modeller has yet achieved this. Unfortunately, this simplification does severely limit the allowable distributions of \mathbf{B}_0 . That is, to ensure that we are perturbing about an equilibrium configuration, we must satisfy $\nabla \times (\mathbf{J}_0 \times \mathbf{B}_0) = 0$. This, in turn, requires that \mathbf{B}_0 is of the form

$$\begin{aligned} \mathbf{B}_0 &= (B_x(x, y), B_y(x, y), B_z), \\ B_z &= \text{constant}, \end{aligned} \tag{5}$$

Our final assumption relates to the aspect ratio of the liquid layers. We shall use the shallow water approximation that $kh \ll 1$, where k is a typical wavenumber. This leads directly to a number of simplifying features, all of which are justified in [3]. To leading order in kh , it may be

shown that: (a) \mathbf{j} is vertical in the cryolite; (b) \mathbf{j} is horizontal in the aluminium and is uniformly distributed across that layer; (c) the perturbed Lorentz force acting on the cryolite may be neglected; (d) the velocity in each layer is uniform in z and horizontal; (e) the dominant contribution to the perturbed Lorentz force in the aluminium is $\mathbf{j} \times (B_z \hat{\mathbf{e}}_z)$. These are illustrated in Figure 3.

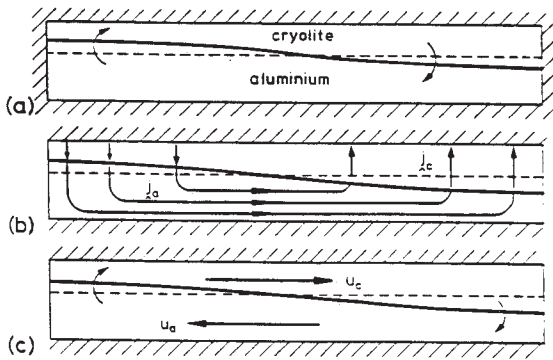


Figure 3: A long wavelength disturbance of the interface results in a perturbed current flow \mathbf{j} , which is largely vertical in the cryolite and horizontal in the aluminium. It also results in a ‘sloshing’ motion in the two liquids which is largely horizontal.

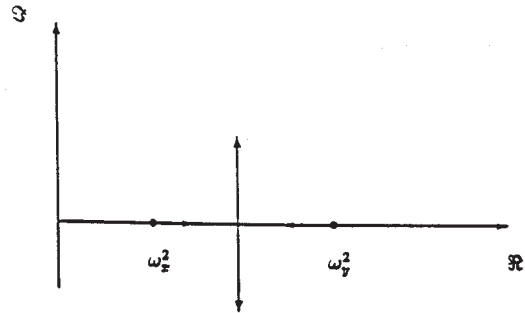


Figure 4: Variations of ω^2 with ω_B .

The Shallow-Water Equation of Davidson & Lindsay

We now summarize the new, shallow-water equation for interfacial waves developed by Davidson & Lindsay [3]. We start with conventional shallow-water theory. This is a two-dimensional, horizontal equation of motion:

$$\rho \frac{\partial \mathbf{u}_H}{\partial t} + \rho g \nabla \eta = -\nabla P_0 + \mathbf{F} . \quad (6)$$

Here \mathbf{u}_H is a two-dimensional velocity field. Next, we replace \mathbf{u}_a and \mathbf{u}_c by the volume fluxes $\mathbf{q}_a = H \mathbf{u}_a$ and $\mathbf{q}_c = -h \mathbf{u}_c$. Also, by virtue of condition (c) in the second section, we may take $\mathbf{F}_c = 0$ (to leading order in kH). Our governing equations now become

$$\frac{\rho_c}{h} \frac{\partial \mathbf{q}_c}{\partial t} - \rho_c g \nabla \eta = \nabla P_0 , \quad (7)$$

$$\frac{\rho_a}{h} \frac{\partial \mathbf{q}_a}{\partial t} + \rho_a g \nabla \eta = -\nabla P_0 + \mathbf{F}_a, \quad (8)$$

$$\nabla \cdot \mathbf{q}_c = \nabla \cdot \mathbf{q}_a = -\frac{\partial \eta}{\partial t}. \quad (9)$$

Equation (9) is a statement of conservation of volume. We now perform a Helmholtz decomposition on \mathbf{q} :

$$\mathbf{q} = \mathbf{q}_R + \mathbf{q}_P.$$

That is, we divide \mathbf{q} into a solenoidal, rotational part and an irrotational component of finite divergence. Evidently, \mathbf{q}_R is zero in the electrolyte, while \mathbf{q}_P is the same in both layers. We now rewrite (7) and (8) in terms of \mathbf{q}_P and \mathbf{q}_R , eliminate P_0 by adding the equations, and express η in terms of \mathbf{q}_P . The resulting equation of motion is

$$\bar{\rho} \frac{\partial^2 \mathbf{q}_P}{\partial t^2} - \Delta \rho g \nabla^2 \mathbf{q}_P = \frac{\partial \mathbf{F}_a}{\partial t} - \frac{\rho_a}{H} \frac{\partial^2 \mathbf{q}_R}{\partial t^2} \quad (10)$$

where $\bar{\rho} = \rho_c/h + \rho_a/H$ and $\Delta \rho = \rho_a - \rho_c$. Note that, when the Lorentz force is zero, we recover the conventional equation for interfacial waves in the shallow-water limits in which waves travel with phase speed:

$$c^2 = \Delta \rho g / \bar{\rho}. \quad (11)$$

We now evaluate \mathbf{j}_a , and hence \mathbf{F}_a , using the long-wavelength approximation of the second section. It is shown in [3] that

$$\frac{\partial \mathbf{j}_H}{\partial t} = -\frac{J_0}{hH} \mathbf{q}_P. \quad (12)$$

Substituting for \mathbf{F}_a we obtain

$$\frac{\partial^2 \mathbf{q}_P}{\partial t^2} - c^2 \nabla^2 \mathbf{q}_P = \omega_B^2 [\hat{\mathbf{e}}_z \times \mathbf{q}_P]_P \quad (13)$$

where $\omega_B^2 = J_0 B_z / \bar{\rho} h H$. The subscript P on the bracket implies that we take only the irrotational component of $\hat{\mathbf{e}}_z \times \mathbf{q}_P$. This is the new wave equation of Davidson & Lindsay. It differs from previous shallow-water descriptions of the interfacial waves in that the Lorentz force is expressed explicitly in terms of the motion.

The shallow-water equation (13) supports both travelling waves and standing waves. It is shown [3] that the travelling-wave solutions of (13) are unstable and that the instability mechanism is different to (and simpler than) that of the travelling waves previously studied. A simpler version of (13) may be obtained if we introduce potentials for \mathbf{q}_P and $\mathbf{F}_P = \mathbf{F}_a - \mathbf{F}_R$:

$$\mathbf{q}_P = \nabla \phi, \quad \nabla \phi \cdot \mathbf{n} = 0$$

$$\frac{\partial \mathbf{F}_P}{\partial t} = \bar{\rho} \nabla \Phi, \quad \nabla \phi \cdot \mathbf{n} = (\nabla \phi \times \mathbf{n})_z$$

Then (13) becomes

$$\begin{aligned} \frac{\partial^2 \phi}{\partial t^2} - c^2 \nabla^2 \phi &= \omega_B^2 \Phi = c^2 k_B^2 \Phi, \\ \nabla^2 \Phi &= 0 \end{aligned} \tag{14}$$

where k_B is defined as ω_B/c .

Unstable Standing Waves

In standing-wave models, the aluminium reduction cell is assumed to be a finite rectangular tank. The disturbed interface, as formulated by Sneyd and Wang [10] and others, is expressed as a combination of gravity-wave modes:

$$\begin{aligned} \eta(x, y, t) &= \\ \sum_{m,n=0}^{\infty} \hat{\eta}_{mn}(t) \cos\left(\frac{m\pi x}{L_x}\right) \cos\left(\frac{n\pi y}{L_y}\right), \end{aligned} \tag{15}$$

L_x and L_y representing the horizontal dimensions of the box. Carrying out the appropriate expansion and truncating the system at a suitably small wavenumber, we may express the wave equation (14) in matrix form:

$$\ddot{\mathbf{x}} + \Omega_g \mathbf{x} = \omega_B^2 \mathbf{K} \mathbf{x}, \tag{16}$$

where Ω_g is a diagonal matrix of the squares of the gravitational frequencies, ω_{gi}^2 , and

$$\omega_B^2 = J_0 B_z / \bar{\rho} H.$$

The interaction matrix, \mathbf{K} , is sparse and skew-symmetric (see [3] for a description of \mathbf{K}).

Let us consider the eigenvalue problem represented by (16):

$$(\Omega_g - \omega_B^2 \mathbf{K}) \mathbf{x} = \lambda \mathbf{x}; \quad \lambda = \omega^2 \tag{17}$$

Of course, instability corresponds to complex values of λ . Suppose that \mathbf{x} is truncated after N modes and that the diagonal elements of Ω_g are arranged in order of increasing frequency, from ω_{g1}^2 to ω_{gN}^2 . Then we may show that the eigenvalues, λ_i , have the following general properties:

- (a) $\omega_{g1}^2 \leq \Re(\lambda) \leq \omega_{gN}^2$;
- (b) $\sum \lambda_i = \sum \omega_{gi}^2$;
- (c) λ_i are zero or purely complex if $\omega_B^2 \gg \omega_{gN}^2$.

These properties are sufficient to define the general behaviour of λ . The first follows from the skew-symmetry of \mathbf{K} . That is, if \bar{x}_i is the complex conjugate of x_i , then

$$\sum_i (\omega_{gi}^2 - \lambda) x_i^2 = \omega_B^2 \sum_i \sum_j K_{ij} x_j \bar{x}_i .$$

If we normalise the eigenvectors to have unit magnitude and take the complex conjugate of the transpose of this equation, we obtain

$$\Re(\lambda) = \sum \omega_{gi}^2 x_i^2 .$$

Condition (a) then follows. Condition (b), on the other hand, arises from the fact that the sum of the eigenvalues equals the trace of $\Omega_g - \omega_B^2 \mathbf{K}$, while condition (c) is a standard result for skew-symmetric matrices.

The situation is therefore clear. As ω_B is increased, the eigenvalues move along the real axis but remain within the limits: $\omega_{g1}^2 < \lambda < \omega_{gN}^2$. At some critical value of ω_B , two or more eigenvalues become complex (an inevitable consequence of condition (c)) and do so in the form of complex conjugate pairs (condition (b)). However, the real part of the complex eigenvalues remain bounded by the smallest and largest gravitational frequency of the truncated set of modes (condition (a)). Condition (c) is enough to guarantee that the cell becomes stable at sufficiently high values of ω_B (see Figure 4). This is discussed in more detail in [3] and [4].

Active Control of the Instability

Our dynamic equation (16) is potentially important in developing a means of controlling the instability. It allows us to predict where the moving interface will be before it gets there. That is, if we know the instantaneous position of the interface $\eta(t)$, as well as its time derivative, then we predict the position of the interface at some future time by solving (16). But we

can estimate η and $\dot{\eta}$ by monitoring the anode voltage and so, within some margin error, we can continuously predict the future location of the interface. Now to suppress the instability we must counter the horizontal correct perturbations induced by the wave in the aluminium (see Figure 3). In principle this may be done by redistributing the current feed into the different anode blocks (by varying external resistances placed in line with each block) or by tilting the anode assembly. In either case we must ensure that the externally induced horizontal current fluctuations (in the aluminium) are such as to eliminate, rather than accentuate, the current perturbations induced by the interfacial wave. Knowing where the interface will be ahead of time is important here, as it means that the cell control system can keep abreast of the wave, rather than continuously trying to keep up with it. In a formal sense we may replace our matrix equation of motion by

$$\ddot{\mathbf{x}} + \Omega_g \mathbf{x} = \omega_B^2 \mathbf{K} (\mathbf{x} + \mathbf{y})$$

where \mathbf{y} is our control parameter (say the tilting of the anode). We can relate \mathbf{y} at a time t to measurements of \mathbf{x} at a previous time $t - \tau$.

$$\mathbf{y}(t) = f(\mathbf{x}(t - \tau))$$

The problem now becomes one of choosing f so that the wave is stabilized. This is the focus of our current research.

Conclusions

A new wave equation for the interface in aluminium reduction cells has been developed from shallow-water theory by Davidson & Lindsay [3]. This equation is valid regardless of the existence or form of boundaries. In the case of rectangular lateral boundaries, the model leads to the (potentially unstable) standing waves of Sneyd and Wang [10]. When an infinitely long channel is considered, we discover a new set of unstable travelling waves. This new model offers one way of developing an active control system for cells.

References

- (1) V. Bojarevics and M. V. Romerio. Long waves instability of liquid metal-electrolyte interface in aluminium electrolysis cells: A generalization of Sele's criterion. *European Journal of Mechanics B*, 13:33-56, 1994.
- (2) P. A. Davidson. An energy analysis of unstable, aluminium reduction cells. *European Journal of Mechanics B*, 13:15-32, 1994.
- (3) P. A. Davidson and R. I. Lindsay. Stability of interfacial waves in aluminium reduction cells. *Journal of Fluid Mechanics*, 1998, to appear.
- (4) P. A. Davidson and R. I. Lindsay. A new model of interfacial waves in aluminium reduction cells. *TMS Conference*, Florida, U.S.A., 1997.
- (5) R. J. Moreau and D. Ziegler. Stability of aluminium cells: A new approach. *Light Metals*, pages 359-364, 1986.
- (6) M. Segatz and C. Droste. Analysis of magnetohydrodynamic instabilities in aluminium reduction cells. *Light Metals*, pages 313-322, 1994.
- (7) T. Sele. Instabilities of the metal surface in electrolyte alumina reduction cells. *Metallurgical Transactions B*, 8B:613-618, 1977.
- (8) A. D. Sneyd. Stability of fluid layers carrying a normal electric current. *Journal of Fluid Mechanics*, 236:111-126, 1992.
- (9) A. D. Sneyd. Interfacial instabilities in aluminium reduction cells. *Journal of Fluid Mechanics*, 236:111-126, 1992.
- (10) A. D. Sneyd and A. Wang. Interfacial instability due to MHD mode coupling in aluminium reduction cells. *Journal of Fluid Mechanics*, 263:343-359, 1994.
- (11) N. Urata. Magnetics and metal pad instability. *Light Metals*, pages 581-589, 1985.